PHYSICAL REVIEW B **90**, 165111 (2014)

Structural and magnetic characterization of iron oxyselenides $Ce_2O_2Fe_2OSe_2$ and $Nd_2O_2Fe_2OSe_2$

E. E. McCabe,[1,2,*] A. S. Wills,[3] L. Chapon,[4,5] P. Manuel,[5] and J. S. O. Evans[2,†]
[1]*School of Physical Sciences, University of Kent, Canterbury, CT2 7NH, United Kingdom*
[2]*Department of Chemistry, Durham University, Durham DH1 3LE, United Kingdom*
[3]*Department of Chemistry, University College London, 20 Gordon Street, London, WC1H 0AJ, United Kingdom*
[4]*Diffraction Group, Institute Laue Langevin, 71 Avenue des Martyrs, 38000 Grenoble, France*
[5]*ISIS Facility, Rutherford Appleton Laboratory, Chilton Didcot, OX11 0QX, United Kingdom*
(Received 4 August 2014; published 9 October 2014)

We present here an investigation of the magnetic ordering in the Mott insulating oxyselenide materials $Ln_2O_2Fe_2OSe_2$ (Ln = Ce, Nd). Neutron powder diffraction data are consistent with a noncollinear multi-k ordering on the iron sublattice structure and analysis indicates a reduced magnetic correlation length perpendicular to the $[Fe_2O]^{2+}$ layers. The magnetic role of the Ln^{3+} cations is investigated and Ce^{3+} moments are found to order at $T \leqslant 16$ K.

DOI: 10.1103/PhysRevB.90.165111 PACS number(s): 75.40.−s, 75.25.−j

I. INTRODUCTION

The discovery of iron-based superconductivity [1] in several mixed anion systems has driven research to understand the magnetism of these materials which is related to their superconducting behavior [2]. The 1111 family of iron-based superconductors derive from LnFeAsO (Ln = trivalent lanthanide) and adopt the ZrCuSiAs- structure [3], composed of alternating layers of antifluorite-like edge-linked $FeAs_4$ tetrahedra alternating with fluorite-like edge-linked OLn_4 tetrahedra. Although the superconductivity arises in the iron arsenide layers, the Ln^{3+} cation has a significant role in both tuning the superconducting T_c in the doped materials [1,4] and in defining the magnetism of the parent nonsuperconducting materials (such as the spin reorientations in NdFeAsO [5] and PrFeAsO [6]). This has led to much research into the interplay between transition metal and lanthanide magnetic sublattices in these and related mixed-anion systems [7–19].

$La_2O_2Fe_2OSe_2$ was the first member of the "M_2O" (M = transition metal) family of oxyselenide materials reported and adopts a layered structure with fluorite-like $[La_2O_2]^{2+}$ slabs (analogous to those in 1111 iron oxyarsenides) separated by Se^{2-} anions from $[Fe_2O]^{2+}$ sheets (Fig. 1) [20]. The Fe^{2+} cations are coordinated by two O(2) ions within these anti-CuO_2 sheets, and by four Se^{2-} ions above and below the sheets, forming a network of face-shared FeO_2Se_4 trans-octahedra. Much research has been carried out to understand the exchange interactions and magnetic ordering present in these $[Fe_2O]^{2+}$ sheets [21]. $La_2O_2Fe_2OSe_2$ orders antiferromagnetically (AFM) below ∼90 K [22] and two magnetic structures have been discussed: a 2-k model first proposed for $Nd_2O_2Fe_2OSe_2$ [23] and a collinear model [10,22]. Recent work suggests that the 2-k model is the more likely [24–26]. In this magnetic structure (Fig. 1), both next-nearest-neighbor (NNN) interactions (ferromagnetic $J_2 \sim 95^\circ$ Fe–Se–Fe interactions, and AFM $J_{2'}$ 180° Fe–O–Fe interactions) are fully satisfied. Interestingly, a similar 2-k model, composed of perpendicular AFM chains, has been predicted for the FeAs sheets in iron arsenides and oxyarsenides [27,28]. The recent studies on $La_2O_2Fe_2OSe_2$ indicated the presence of antiphase boundaries or stacking faults perpendicular to the stacking direction and gave evidence for 2D-Ising-like magnetism within these sheets [25]. In the light of this work, it is timely to report a similar analysis on $Ln_2O_2Fe_2OSe_2$ (Ln = Ce, Nd) analogs to test the robustness of the 2-k model to changes in Fe–O bond lengths and to a magnetic moment on the Ln site. We show that neutron powder diffraction (NPD) data are consistent with the proposed 2-k magnetic structure and that much larger magnetic stacking domains are formed with these smaller magnetic lanthanides. In contrast with previous work [10], we show that Ce moments order at low temperatures and that unlike many related oxyarsenide systems, this Ce moment ordering does not cause a reorientation of the Fe^{2+} moments.

II. EXPERIMENTAL DETAILS

5 g each of $Ce_2O_2Fe_2OSe_2$ and $Nd_2O_2Fe_2OSe_2$ were prepared by solid state reaction of CeO_2 (Alfa-Aesar, 99.8%) or Nd_2O_3 (Electronic Materials, 99%), Fe (Aldrich, 99.9%) and Se (Alfa Aesar, 99.999%) powders. For $Nd_2O_2Fe_2OSe_2$, stoichiometric quantities of these reagents were intimately ground by hand using an agate pestle and mortar. The resulting gray powder was pressed to form several pellets of 5 mm diameter. These were placed inside a quartz tube which was evacuated and sealed. This was then heated slowly to 1000 °C, held at this temperature for 12 h, and then cooled in the furnace. For $Ce_2O_2Fe_2OSe_2$, a stoichiometric mixture of reagents was ground together and pressed into pellets which were placed in a quartz tube with an oxygen-getter (Al powder in 10% excess which was physically isolated from the reagents). This tube was evacuated, sealed, slowly heated to 1000 °C, and held at this temperature for 12 h. The reaction tube was then quenched into a bucket of iced water. Both $Ce_2O_2Fe_2OSe_2$ and $Nd_2O_2Fe_2OSe_2$ were formed as black, polycrystalline powders. Preliminary structural characterization was carried out using a Bruker D8 Advance diffractometer fitted with a LynxEye silicon strip detector (step size 0.021°) operating in reflection mode with Cu $K\alpha$ radiation. NPD data were collected on the time of flight (TOF) diffractometer WISH [29] on target station 2 at the ISIS spallation neutron source. The powders were placed in cylindrical 6 mm diameter vanadium cans (to heights of ∼6 cm). For $Ce_2O_2Fe_2OSe_2$, 16 min

---

[*] Corresponding author: e.e.mccabe@kent.ac.uk
[†] Corresponding author: john.evans@durham.ac.uk

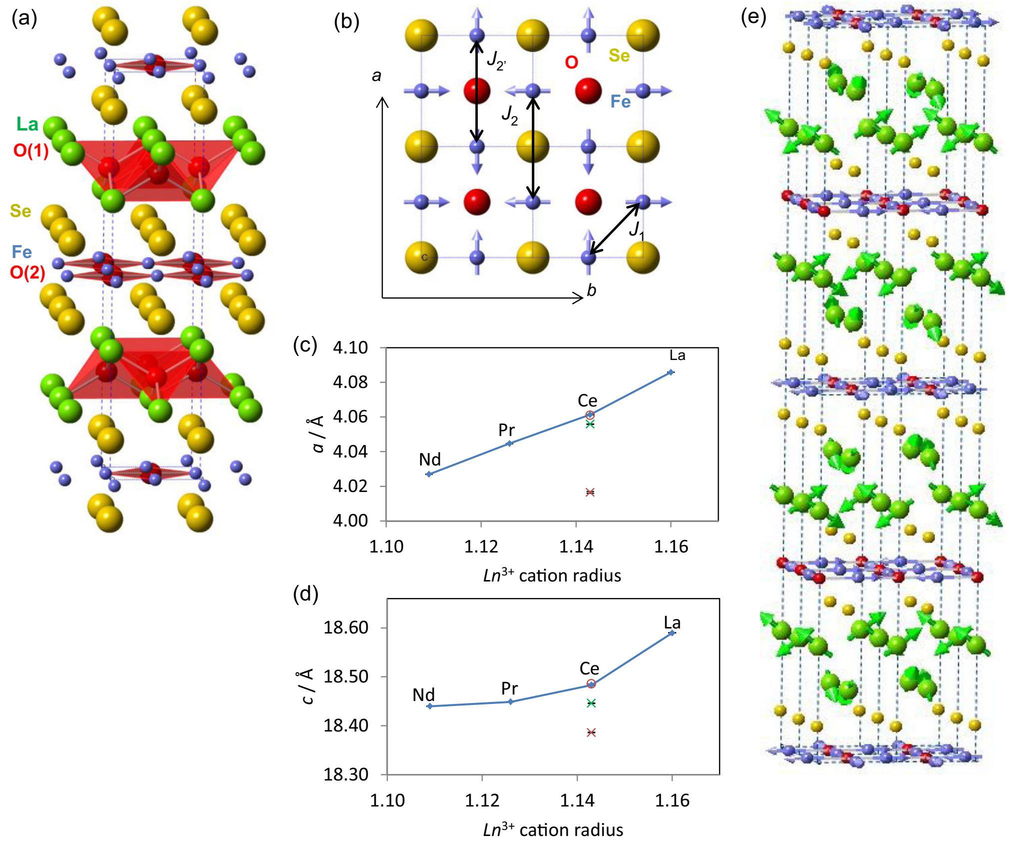

FIG. 1. (Color online) (a) Nuclear cell of $Ln_2O_2Fe_2OSe_2$ with O^{2-}, Se^{2-}, Fe^{2+}, and Ln^{3+} ions in red, yellow, blue, and green, respectively, showing $[Ln_2O_2]^{2+}$ fluorite-like layers built from edge-shared OLn_4 tetrahedra in red; (b) shows the in-plane arrangement of magnetic moments for the 2-*k* model, with O^{2-} (red), Se^{2-} (yellow), and Fe^{2+} (blue) ions shown, and Fe^{2+} moments shown by blue arrows; the three intraplanar exchange interactions J_1, J_2, and $J_{2'}$ are also shown; (c) and (d) show plots of unit cell parameters *a* and *c* for $Ln_2O_2Fe_2OSe_2$ determined from Rietveld analysis using room temperature XRPD data (data in blue are described in this work including quench-cooled $Ce_2O_2Fe_2OSe_2$); data in red are determined for the main (◯) and secondary (×) phases in two phase samples of "$Ce_2O_2Fe_2OSe_2$"; green points are those reported for $Ce_2O_2Fe_2OSe_2$ by Ni *et al.* [10]; (e) illustrates the magnetic ordering of Ce (green) and Fe (blue) moments [O(1) sites are omitted for clarity].

(10 μA h) scans were collected every 4 K on cooling from 120 K to 8 K and a final 25 min (15 μA h) scan was collected at 1.5 K. For $Nd_2O_2Fe_2OSe_2$, several 16 min (10 μA h) scans were collected between 1.5 K and 12 K followed by a further 5 on warming to 300 K. Rietveld refinements [30] were performed using Topas Academic software [31,32]. Sequential refinements were controlled using local subroutines. The high *d*-spacing 59° bank of data (10.5–85.0 ms, 1–8 Å) was used to study the magnetic behavior of the two materials. The nuclear and magnetic refinements were carried out with separate nuclear and magnetic phases (lattice parameters and scale factor of the magnetic phase were constrained to be multiples of the nuclear phase). Magnetic susceptibility was measured using a Magnetic Properties Measurement System (Quantum Design, MPMS). Field-cooled and zero-field-cooled data were collected on warming from 2 K to 292 K at 5 K intervals in an applied magnetic field of 1000 Oe. Field sweep measurements to $\pm5\times10^4$ Oe were made at 292 K and at 12 K. Scanning electron microscopy for compositional analysis of $Ce_2O_2Fe_2OSe_2$ samples used a Hitachi SU-70 FEG electron microscope. Back-scattered electron (BSE) images were collected with a YAG BSE detector to investigate compositional homogeneity and energy-dispersive x-ray analysis (EDX) measurements were made over areas of the sample and at 65–100 points on each sample.

III. RESULTS

The synthesis method described gave a single-phase sample of $Nd_2O_2Fe_2OSe_2$ by x-ray and neutron analysis (see Supplemental Material [33]). Quenching the sealed reaction tube of $Ce_2O_2Fe_2OSe_2$ from the reaction temperature into iced water gave an almost single-phase sample of $Ce_2O_2Fe_2OSe_2$ (NPD data revealed the presence of ∼3% by weight of a second phase similar to the main phase which was included in refinements). See Supplemental Material [33] for further analyses. Rietveld refinements using NPD data for both $Ln = \mathrm{Ce}$, Nd phases are in good agreement with the nuclear structure previously reported [10]. Refining site occupancies (with *Ln* site fully occupied) gave compositions close to stoichiometric ($Ce_2O_{1.99(1)}Fe_{2.00(1)}O_{0.99(1)}Se_{2.0(1)}$ and $Nd_2O_{1.93(1)}Fe_{1.96(1)}O_{0.913(9)}Se_{2.05(1)}$). Site occupancies were fixed at unity for subsequent refinements. These $Ln = \mathrm{Ce}$, Nd phases can be compared with $Ln = \mathrm{La}$, Pr analogs and the expected decrease in unit cell parameters with decreasing Ln^{3+} ionic radii is observed (1).

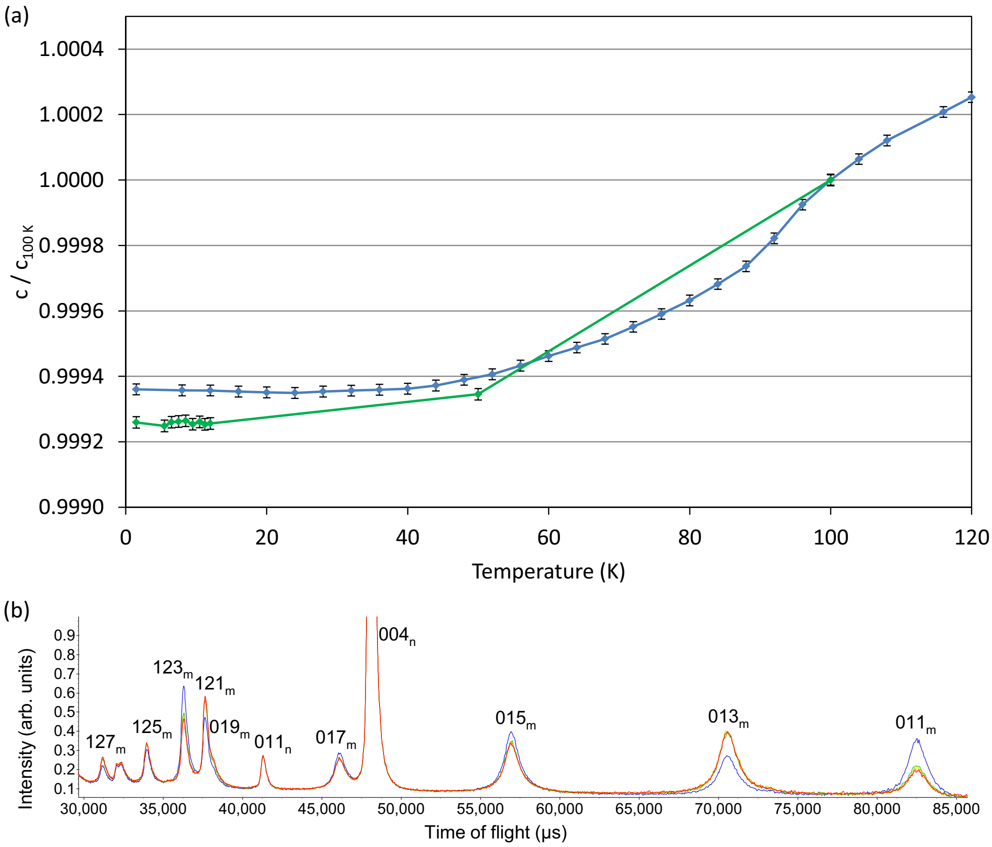

FIG. 2. (Color online) (a) Plots of unit cell parameter $c/c_{100\,\mathrm{K}}$ for $Ln_2O_2Fe_2OSe_2$ (Ln = Ce, Nd) from sequential Rietveld refinements using NPD data; data are shown in blue and green for Ce and Nd analogs, respectively; (b) NPD data (59° bank from WISH TOF diffractometer) collected for $Ce_2O_2Fe_2OSe_2$ at 1.5 K (dark blue), 8 K (green), 12 K (yellow), 16 K (orange), and 20 K (red). *hkl* indices of key reflections are given and subscripts m and n refer to the magnetic and nuclear phases, respectively.

Sequential Rietveld refinements using $Ce_2O_2Fe_2OSe_2$ data collected on cooling from 120 K reveal a decrease in unit cell volume on cooling (similar behavior is observed for $Nd_2O_2Fe_2OSe_2$). For both Ln = Ce, Nd analogs, a more rapid decrease of c unit cell parameter is observed immediately below T_N [Fig. 2(a)] which is similar to that observed for $La_2O_2Fe_2OSe_2$ [22].

Additional Bragg reflections were observed in NPD data collected for both materials below T_N [92.3(2) K for $Ce_2O_2Fe_2OSe_2$] and are consistent with the 2-k magnetic structure reported for $La_2O_2Fe_2OSe_2$ [25]. For the Ce sample, at 96 K, some diffuse scattering is observed at a similar d spacing to the most intense magnetic Bragg reflection (see Supplemental Material [33]), suggesting some two-dimensional short-range ordering immediately above the transition to a three-dimensional AFM phase. Data were not collected at sufficiently small temperature increments to investigate this for $Nd_2O_2Fe_2OSe_2$.

Significant anisotropic peak broadening of magnetic Bragg reflections was observed for both Ce and Nd phases, similar to that observed for $La_2O_2Fe_2OSe_2$ [25]. This could be modeled with an expression for antiphase boundaries perpendicular to the c axis [34,35], which gave a significantly improved fit to the data (Fig. 3 and Supplemental Material [33]) and suggested magnetic correlation lengths along c, ξ_c, at 1.5 K of 87(1) Å and 86(2) Å for Ce and Nd analogs, respectively.

For $Ce_2O_2Fe_2OSe_2$, the 2-k model with ordered Fe^{2+} moments gives a good fit to NPD data down to ∼24 K but a change in relative intensities of magnetic Bragg reflections is observed at lower temperatures [Fig. 2(b)] and whilst no additional reflections appear, the 24 K model gives a poor fit at 1.5 K [Fig. 3(c)].

The low-temperature magnetic structure was investigated using the symmetry-adapted mode approach [36] where the magnetic structure is described in terms of the parent crystal structure with a number of symmetry-adapted magnetic ordering modes, or basis vectors, imposed on it. The amplitudes of these modes or basis vectors can be refined to model various magnetic structures. The approach of directly refining the contributions of the different magnetic basis vectors is similar to that originally developed in SARAh [37]. Mode inclusion analysis [25,38] (see Supplemental Material [33] for more details) indicated no change in the Fe moment arrangement on cooling. A good fit could, however, be obtained with an ordered moment on Ce sites. The in-plane component of the Ce moments is of the same symmetry as the Fe ordering, but allowing the Ce moments to cant out of plane improves the fit further [for refinement using both 153° and 59° banks of data, R_{wp} decreases from 5.589% to 5.127% for one additional parameter; see Supplemental Material [33] for comparison with Fig. 3(d)]. A combined refinement using both high resolution data (153° bank) and long d-spacing data (59° bank)

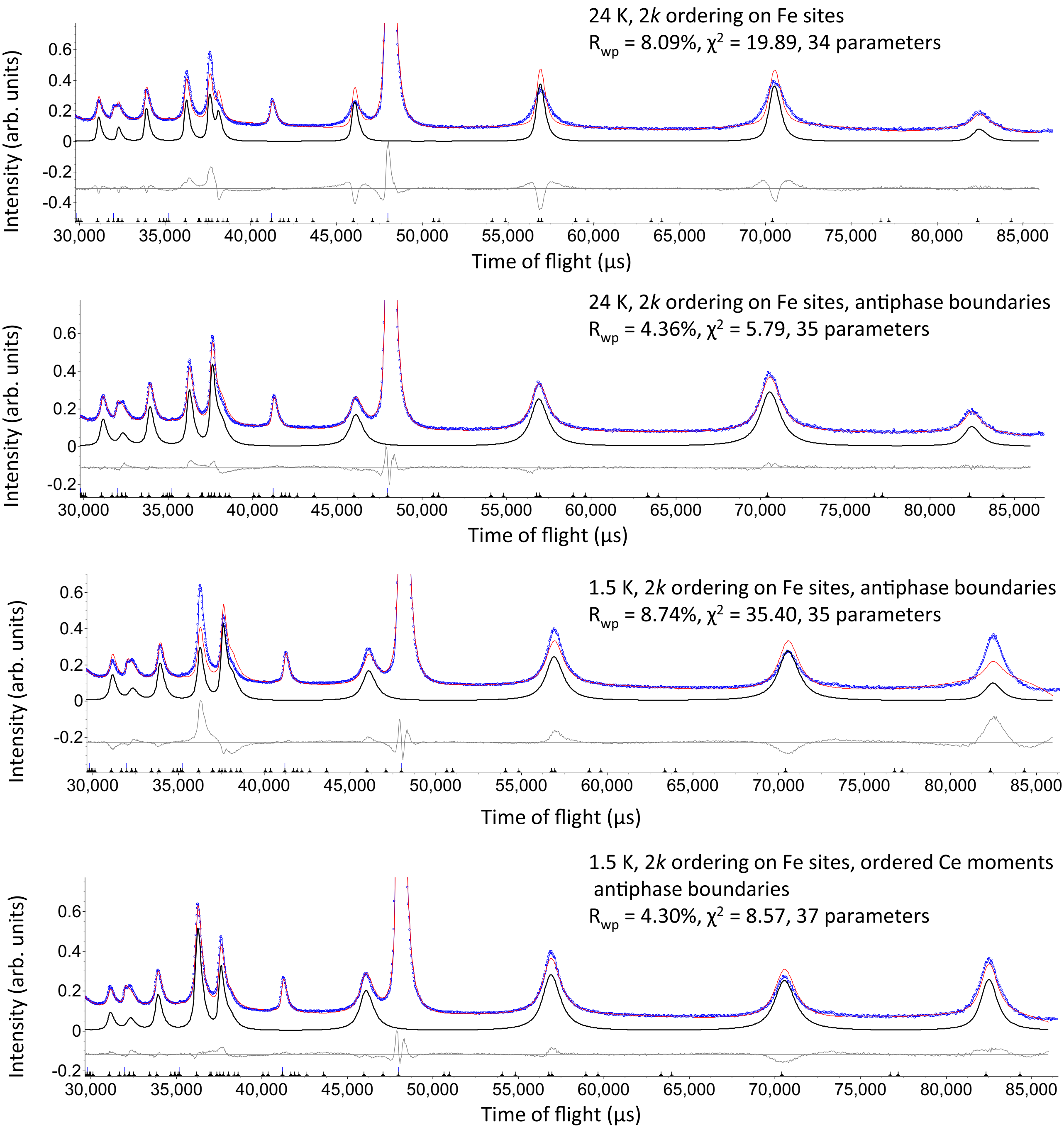

FIG. 3. (Color online) Rietveld refinement profiles using NPD data (59° bank from WISH TOF diffractometer) of $Ce_2O_2Fe_2OSe_2$ focusing on the magnetic reflections with 2-k magnetic ordering model on Fe^{2+} sublattice, showing (a) refinement at 24 K with the same peak shape for both magnetic and nuclear phases; (b) refinement at 24 K including antiphase boundaries for the magnetic phase; (c) refinement at 1.5 K with antiphase boundaries for the magnetic phase (only Fe moments ordered), and (d) refinement at 1.5 K with antiphase boundaries for the magnetic phase and ordering of both Fe and Ce moments. Observed and calculated (upper) and difference profiles are shown by blue points, and red and gray lines, respectively. Magnetic intensity is highlighted by solid black line.

was carried out using data collected at 1.5 K and final refinement profiles are shown in Fig. 4 and refinement details are given in Table I.

Sequential Rietveld refinements carried out using only data from the 59° bank (which is the more sensitive to magnetic ordering) collected on cooling $Ce_2O_2Fe_2OSe_2$ indicate no change in the magnetic correlation length along c and the onset of magnetic order on the Fe sites in the Ce phase can be described by critical behavior with the exponent $\beta_{Fe} = 0.11(1)$ (Fig. 5). Moments on Ce sites remain close to zero until $T \leqslant 16$ K.

Magnetic susceptibility measurements on both $Ce_2O_2Fe_2OSe_2$ and $Nd_2O_2Fe_2OSe_2$ are included as Supplemental Material [33]. They were consistent with

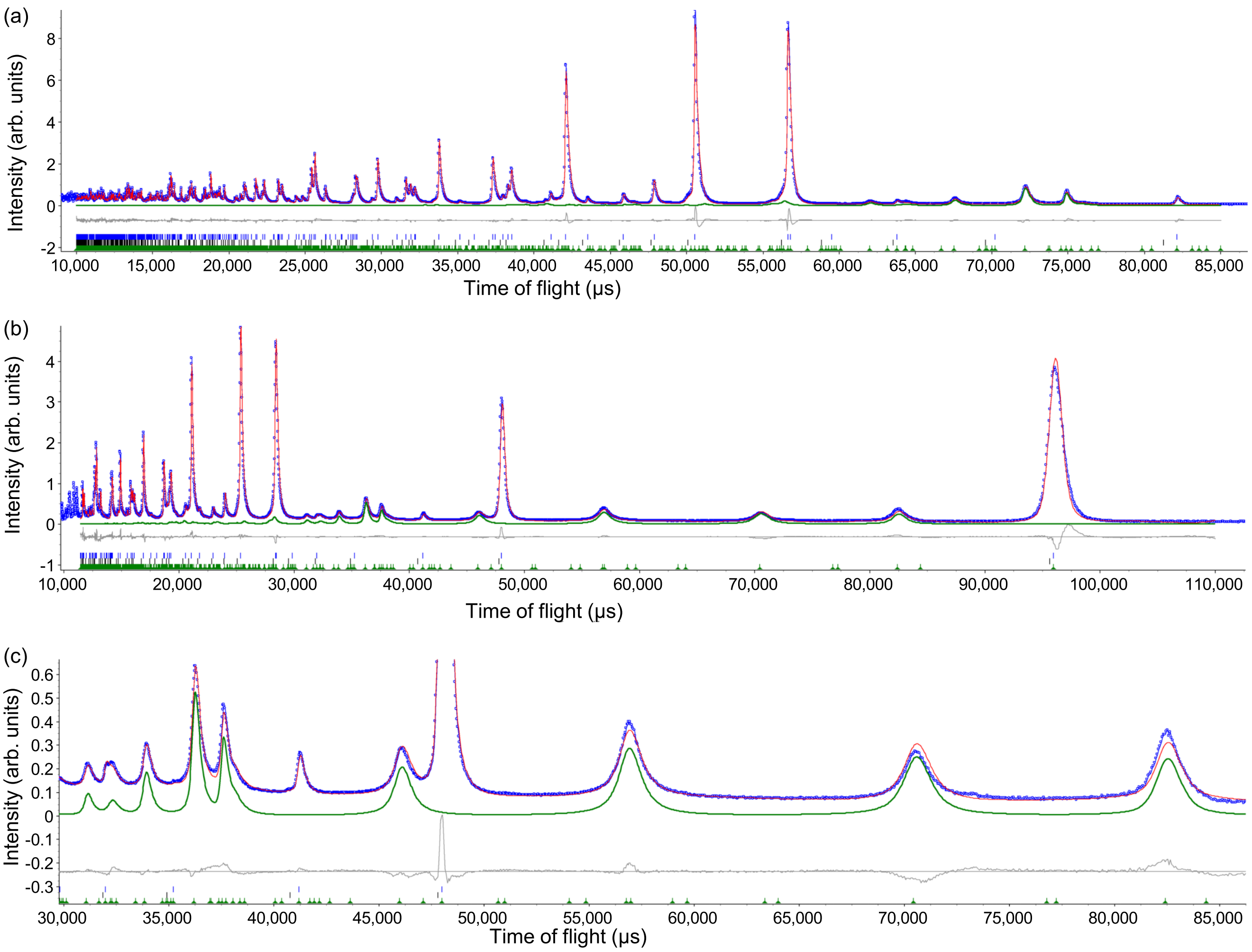

FIG. 4. (Color online) Rietveld refinement profiles from combined refinement (a) using 153° bank data and (b) 59° bank data collected for $Ce_2O_2Fe_2OSe_2$ at 1.5 K; (c) shows the higher d-spacing region of 59° bank data highlighting the magnetic reflections. Observed and calculated (upper) and difference profiles are shown by blue points, and red and gray lines, respectively. Magnetic intensity is highlighted by solid green line.

those reported by Ni *et al.* [10], showing a slight cusp in susceptibility at ~90 K, which is attributed to long range magnetic ordering of the Fe sublattice.

TABLE I. Details from Rietveld refinement using NPD data collected at 1.5 K for $Ce_2O_2Fe_2OSe_2$. The refinement was carried out with the nuclear structure described by space group $I4/mmm$ with $a = 4.0526(2)$ Å and $c = 18.440(1)$ Å. The magnetic scattering was fitted by a second magnetic-only phase with a, b, and c unit cell parameters constrained to be twice those of the nuclear phase; $R_{wp} = 5.127\%$, $R_p = 5.070\%$, and $\chi^2 = 13.06$.

Atom	Site	x	y	z	$U_{\mathrm{iso}} \times 100$ (Å^2)	Moment (μ_B)
Ce	$4e$	0.5	0.5	0.184 71(6)	0.52(4)	0.89(1) (xy) 0.54(1) (z)
Fe	$4c$	0.5	0	0	0.71(2)	3.32(1)
Se	$4e$	0	0	0.097 55(4)	0.40(3)	
O1	$4d$	0.5	0	0.25	0.70(3)	
O2	$2b$	0.5	0.5	0	0.85(4)	

IV. DISCUSSION

The difficulty in preparing a single phase sample of $Ce_2O_2Fe_2OSe_2$ may be due to the variable oxidation state of cerium, with both +3 and +4 oxidation states accessible. The secondary phase present in initial syntheses has a smaller unit cell than the almost single-phase material and is thought to contain some Ce^{4+} and vacancies on the Fe^{2+} sites (although we cannot rule out the possibility of some excess oxide ions on interstitial sites). This is similar to reports on the Ce-Cu-O-S system for which both $(Ce^{3+}, Ce^{4+})Cu_{1-x}OS$ and the stoichiometric $Ce^{3+}CuOS$ can be prepared [39]. Based on other Ln systems, the unit cell parameters for the single-phase sample of $Ce_2O_2Fe_2OSe_2$ are consistent with those expected for Ce^{3+} (see Fig. 1), suggesting that this phase is close to stoichiometric. Site occupancies from Rietveld analysis of the NPD data are consistent with this.

Variable temperature NPD data show that both Ln = Ce, Nd phases remain tetragonal at low temperatures, unlike $Ln_2O_2Mn_2OSe_2$, Ln = La, Pr, for which low-temperature tetragonal-orthorhombic phase transitions have been reported [40]. These transitions for the Mn phases are thought to

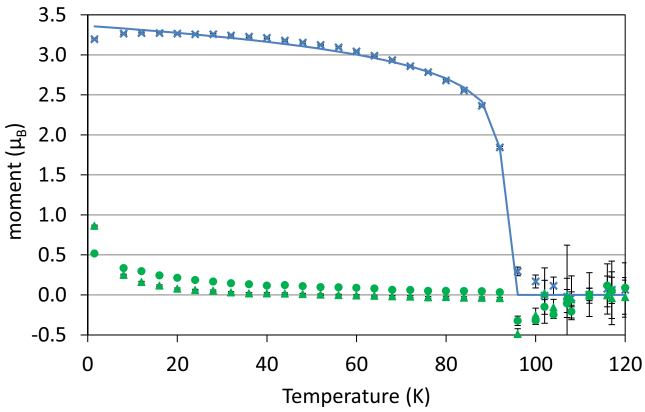

FIG. 5. (Color online) Evolution of magnetic moment on Fe sites (blue crosses) and on Ce sites in the *ab* plane (open green triangles) and along *c* (green crosses) on cooling $Ce_2O_2Fe_2OSe_2$; solid blue line shows fit to function $M_T = M_0[1 - (\frac{T}{T_N})]^{\beta}$ representing critical behavior of Fe ordering with $M_0 = 3.36(4)\mu_B$, $T_N = 92.3(2)$ K, and $\beta_{Fe} = 0.11(1)$.

involve the in-plane O(2) site [40] and may reflect the frustrated Mn–O(2)–Mn J_2 interactions present in the magnetically ordered phase below T_N. This is in contrast to the 2-*k* magnetic structure observed for $Ln_2O_2Fe_2OSe_2$ (Ln = La, Ce, Nd) with in-plane Fe–O(2)–Fe J_2 and Fe–Se–Fe J_2 interactions satisfied [25]. The absence of distortions from tetragonal symmetry is consistent with predictions from theoretical work that such a 2-*k* structure might suppress any lattice distortions [27]. The contraction in unit cell parameter *c* at the onset of AFM ordering is similar for all $Ln_2O_2Fe_2OSe_2$ analogs [Fig. 2(a)] and less pronounced than for Mn-containing materials.

The observation of the same 2-*k* magnetic structure across the series $Ln_2O_2Fe_2OSe_2$ (Ln = La, Ce, Nd) suggests that this ordering pattern is robust with respect to chemical pressure (the ∼4% decrease in Ln ionic radii from Ln = La to Ln = Ce [41] results in an ∼4% decrease in unit cell volume [10], with a relatively larger contraction in the *ab* plane). This is consistent with the low level of frustration in this 2-*k* magnetic structure, with both NNN J_2 and $J_{2'}$ interactions satisfied. We note that the magnetic correlation lengths ξ_c for $Ce_2O_2Fe_2OSe_2$ and $Nd_2O_2Fe_2OSe_2$ are almost twice that found for $La_2O_2Fe_2OSe_2$ [$\xi_c = 45(3)$ Å [25]]. The greater magnetic correlation length along *c* in these Ln = Ce, Nd analogs might be due to their decreased interlayer separation.

The ordered moments on the Fe sites reported here for $Ln_2O_2Fe_2OSe_2$ [$3.32(1)\mu_B$ and $3.18(1)\mu_B$ at 1.5 K for Ln = Ce, Nd, respectively] are larger than those reported previously [$2.23(3)\mu_B$ per Fe site at 5 K in $Pr_2O_2Fe_2OSe_2$ [10]] presumably as a result of improved fitting of the anisotropically broadened magnetic Bragg reflections and are very similar to that found for $La_2O_2Fe_2OSe_2$ [$3.50(5)\mu_B$ at 2 K] [25]. The evolution of the Fe moment on cooling observed in $Ce_2O_2Fe_2OSe_2$ (and the β exponent β_{Fe} obtained) is very similar to that reported for $La_2O_2Fe_2OSe_2$ [$\beta_{Fe} = 0.122(1)$] and consistent with 2D-Ising-like behavior reported for several related systems [23,25]. The diffuse scattering observed only 4 K above T_N for $Ce_2O_2Fe_2OSe_2$ is also consistent with the 2D-like spin fluctuations before the onset of 2D magnetic order. As noted by Ni *et al.*, the lack of a clear maximum in susceptibility data for Ln = Ce, Nd analogs (and the small entropy release observed in their careful heat capacity measurements) again suggests a 2D to 3D magnetic transition [10].

Ordering of Ce moments at low temperature in $Ce_2O_2Fe_2OSe_2$ has not been reported previously. This may reflect the difficulty in preparing stoichiometric samples of Ce-containing transition metal oxychalcogenides which can easily contain transition metal vacancies and diamagnetic Ce^{4+} cations, or the difficulty in detecting small ordered moments [$1.08(1)\mu_B$ per Ce site observed here] which only develop at very low temperatures. The Ce moment obtained is consistent with that expected for a Ce^{3+} doublet ground state ($1\mu_B$) [15] and similar to that observed in related $Ce_2O_2FeSe_2$ [$1.14(4)\mu_B$ at 4 K] [11] and CeFeAsO [$0.83(2)\mu_B$ at 1.7 K] [42].

Below $T_{N,Ce}$ Ce moments have a similar in-plane arrangement to the Fe moments (Fig. 1), although a significant component is directed along *c*. This is in contrast with related CeMnAsO in which Ce moments lie within the *ab* plane [14,16], consistent with the easy axis along *x* proposed for Ce^{3+} sites in fluoritelike $[Ce_2O_2]^{2+}$ layers in related orthorhombic materials [17]. In CeFeAsO, Ce moments are predominantly within the *ab* plane but a small out-of-plane component has been proposed [42]. This canting of Ce moments away from the easy axis may indicate some Fe–Ce coupling in these iron-based mixed anion systems. We find no evidence of Fe moment reorientation at the onset of Ce^{3+} moment ordering in $Ce_2O_2Fe_2OSe_2$ (which we expect our analysis to be sensitive to, given the relatively large moments on Fe sites). This is in contrast to CeMnAsO [14] and CeFeAsO [13], where some reorientation of transition metal spins has been reported at $T_{N,Ce}$. The lack of any spin reorientation in $Ce_2O_2Fe_2OSe_2$ may reflect the Ising-like nature of the Fe ordering, with the local anisotropy of Fe directing moments oriented along Fe–O(2) bonds and parallel to the expected Ce easy axis. Analysis of the magnetic order in $La_2O_2Fe_2OSe_2$ by Günther *et al.* [24] has shown that the 2-*k* magnetic ordering on the Fe sublattice gives rise to two inequivalent Ln sites. Refinements allowing inequivalent Ce sites did not improve the fit and our data may not be sensitive to this.

V. CONCLUSIONS

In conclusion, we have shown that NPD data for $Ln_2O_2Fe_2OSe_2$ (Ln = Ce, Nd) are consistent with the 2-*k* magnetic structure and, like the La analog, ordering of the Fe^{2+} moments is characterized by 2D-Ising-like spin fluctuations around the critical point. Below 16 K, Ce moments order with a similar 2-*k* arrangement but with a large out-of-plane component. The lack of any reorientation of Fe moments at the onset of Ce spin order may reflect the Ising-like nature of the Fe moments. Canting of Ce moments away from their easy-axis may indicate some Fe–Ce coupling.

ACKNOWLEDGMENTS

We acknowledge STFC, EPSRC (Grant No. EP/J011533/1) for funding. We thank Dmitry Khalyavin (ISIS), Budhika Mendis (Durham), and Leon Bowen (Durham) for assistance and Chris Stock, Efrain Rodriguez, and Mark Green for helpful discussions.

[1] Y. Kamihara, T. Watanabe, M. Hirano, and H. Hosono, J. Am. Chem. Soc. **130**, 3296 (2008).

[2] A. L. Wysocki, D. D. Belashchenko, and V. P. Antipov, Nat. Phys. **7**, 485 (2011).

[3] V. Johnson and W. Jeitschko, J. Solid State Chem. **11**, 161 (1974).

[4] Z.-A. Ren, W. Wu, J. Yang, W. Yi, X.-L. Shen, Z.-C. Li, G.-C. Che, X.-L. Dong, L.-L. Sun, F. Zhou, and Z.-X. Zhao, Chin. Phys. Lett. **25**, 2215 (2008).

[5] W. Tian, W. Ratcliff, M. G. Kim, J.-Q. Yan, P. A. Kienzle, Q. Huang, B. Jensen, K. W. Dennis, R. W. McCallum, T. A. Lograsso, R. J. McQueeney, A. I. Goldman, J. W. Lynn, and A. Kreyssig, Phys. Rev. B **82**, 060514(R) (2010).

[6] D. Bhoi, P. Mandal, P. Choudhury, S. Pandya, and V. Ganesan, J. Appl. Phys. **110**, 113722 (2011).

[7] S. A. J. Kimber, A. H. Hill, Y.-Z. Zhang, H. O. Jeschke, R. Valenti, C. Ritter, I. Schellenberg, W. Hermes, R. Pottgen, and D. N. Argyriou, Phys. Rev. B **82**, 100412(R) (2010).

[8] A. Marcinkova, T. C. Hansen, and J.-W. G. Bos, J. Phys.: Condens. Matter **24**, 256007 (2012).

[9] A. Marcinkova, T. C. Hansen, C. Curfs, S. Margadonna, and J.-W. G. Bos, Phys. Rev. B **82**, 174438 (2010).

[10] N. Ni, S. Jia, Q. Huang, E. Climent-Pascual, and R. J. Cava, Phys. Rev. B **83**, 224403 (2011).

[11] E. E. McCabe, C. Stock, J. Bettis, E. E. Rodriguez, M.-H. Whangbo, and J. S. O. Evans [Phys. Rev. B (to be published)].

[12] H. Maeter, H. Luetkens, Y. G. Pashkevich, A. Kwadrin, R. Khasanov, A. Amato, A. A. Gusev, K. V. Lamonova, D. A. Chervinskii, R. Klingeler, C. Hess, G. Behr, B. Buchner, and H.-H. Klauss, Phys. Rev. B **80**, 094524 (2009).

[13] Q. Zhang, W. Tian, H. Li, J.-W. Kim, J. Yan, R. W. McCallum, T. A. Lograsso, J. L. Zarestky, S. L. Bud'ko, R. J. McQueeney, and D. Vaknin, Phys. Rev. B **88**, 174517 (2013).

[14] C. Lee, E. Kan, H. Xiang, R. K. Kremer, S.-H. Lee, Z. Hiroi, and M.-H. Whangbo, Inorg. Chem. **51**, 6890 (2012).

[15] S. Chi, D. T. Adroja, T. Guidi, R. Bewley, S. Li, J. Zhao, J. W. Lynn, C. M. Brown, Y. Qiu, G. F. Chen, J. L. Lou, N. L. Wang, and P. Dai, Phys. Rev. Lett. **101**, 217002 (2008).

[16] Y. Tsukomoto, Y. Okamoto, K. Matsuhira, M.-H. Whangbo, and Z. Hiroi, J. Phys. Soc. Jpn. **80**, 094708 (2011).

[17] O. V. Gornostaeva, K. V. Lamonova, S. M. Orel, and Y. G. Pashkevich, Low Temp. Phys. **39**, 343 (2013).

[18] A. Jesche, C. Krellner, M. de Souza, M. Lang, and C. Geibel, New J. Phys. **11**, 103050 (2009).

[19] M. A. McGuire, R. P. Hermann, A. S. Sefat, B. C. Sales, R. Jin, D. Mandrus, F. Grandjean, and G. J. Long, New J. Phys. **11**, 025011 (2009).

[20] J. M. Mayer, L. F. Schneemeyer, T. Siegrist, J. V. Waszczak, and B. van Dover, Ang. Chem. Int. Ed. Eng. **31**, 1645 (1992).

[21] H. Kabbour, E. Janod, B. Corraze, M. Danot, C. Lee, M.-H. Whangbo, and L. Cario, J. Am. Chem. Soc. **130**, 8261 (2008).

[22] D. G. Free and J. S. O. Evans, Phys. Rev. B **81**, 214433 (2010).

[23] Y. Fuwa, M. Wakeshima, and Y. Hinatsu, J. Phys.: Condens. Matter **22**, 346003 (2010).

[24] M. Günther, S. Kamusella, R. Sarkar, T. Goltz, H. Luetkens, G. Pascua, S.-H. Do, K.-Y. Choi, H. D. Zhou, and H.-H. Klauss, arXiv:1404.0249.

[25] E. E. McCabe, C. Stock, E. E. Rodriguez, A. S. Wills, J. W. Taylor, and J. S. O. Evans, Phys. Rev. B **89**, 100402(R) (2014).

[26] L. L. Zhao, S. Wu, J. K. Wang, J. P. Hodges, C. Broholm, and E. Morosan, Phys. Rev. B **87**, 020406(R) (2013).

[27] J. Lorenzana, G. Seibold, C. Ortix, and M. Grilli, Phys. Rev. Lett. **101**, 186402 (2008).

[28] G. Giovannetti, C. Ortix, M. Marsman, M. Capone, J. van den Brink, and J. Lorenzana, Nat. Commun. **2**, 398 (2011).

[29] L. C. Chapon, P. Manuel, P. G. Radaelli, C. Benson, L. Perrott, S. Ansell, N. J. Rhodes, D. Raspino, D. Duxbury, E. Spill, and J. Norris, Neutron News **22**, 22 (2011).

[30] H. M. Rietveld, J. Appl. Crystallogr. **2**, 65 (1969).

[31] A. A. Coelho, J. Appl. Crystallogr. **36**, 86 (2003).

[32] A. A. Coelho, *TopasAcademic: General Profile and Structure Analysis Software for Powder Diffraction Data* (Bruker AXS: Karlsruhe, Germany, 2012).

[33] See Supplemental Material at http://link.aps.org/supplemental/10.1103/PhysRevB.90.165111 for further details regarding synthesis, analysis of diffraction data (including mode inclusion analysis), as well as magnetic susceptibility and field sweep measurements.

[34] J.-H. Her, P. W. Stephens, Y. Gao, G. L. Soloveichik, J. Rijssenbeek, M. Andrus, and J.-C. Zhao, Acta Crystallogr., B **63**, 561 (2007).

[35] E. E. McCabe and J. S. O. Evans, Topas wiki user macros, http://topas.dur.ac.uk/topaswiki/doku.php

[36] B. J. Campbell, H. T. Stokes, D. E. Tanner, and D. M. Hatch, J. Appl. Crystallogr. **39**, 607 (2006).

[37] A. S. Wills, Physica B **276–278**, 680 (2000).

[38] A. J. Tuxworth, E. E. McCabe, D. G. Free, S. J. Clark, and J. S. O. Evans, Inorg. Chem. **52**, 2078 (2013).

[39] M. J. Pitcher, C. F. Smura, and S. J. Clarke, Inorg. Chem. **48**, 9054 (2009).

[40] D. G. Free, N. D. Withers, P. J. Hickey, and J. S. O. Evans, Chem. Mater. **23**, 1625 (2011).

[41] R. D. Shannon, Acta Crystallogr. A **32**, 751 (1976).

[42] J. Zhao, Q. Huang, C. de la Cruz, S. Li, J. W. Lynn, Y. Chen, M. A. Green, G. F. Chen, G. Li, Z. Li, J. L. Luo, N. L. Wang, and P. Dai, Nat. Mater. **7**, 953 (2008).